

Promoting Effect of Layered Titanium Phosphate on the Electrochemical and Photovoltaic Performance of Dye-Sensitized Solar Cells

Ping Cheng · Ruihao Chen · Junfei Wang ·
Jianong Yu · Tian Lan · Wanjun Wang ·
Haijun Yang · Haixia Wu · Changsheng Deng

Received: 25 February 2010 / Accepted: 8 May 2010 / Published online: 20 May 2010
© The Author(s) 2010. This article is published with open access at Springerlink.com

Abstract We reported a composite electrolyte prepared by incorporating layered α -titanium phosphate (α -TiP) into an iodide-based electrolyte using 1-ethyl-3-methylimidazolium tetrafluoroborate (EmimBF₄) ionic liquid as solvent. The obtained composite electrolyte exhibited excellent electrochemical and photovoltaic properties compared to pure ionic liquid electrolyte. Both the diffusion coefficient of triiodide (I₃⁻) in the electrolyte and the charge-transfer reaction at the electrode/electrolyte interface were improved markedly. The mechanism for the enhanced electrochemical properties of the composite electrolyte was discussed. The highest conversion efficiency of dye-sensitized solar cell (DSSC) was obtained for the composite electrolyte containing 1wt% α -TiP, with an improvement of 58% in the conversion efficiency than the blank one, which offered a broad prospect for the fabrication of stable DSSCs with a high conversion efficiency.

Keywords Diffusion · Charge transfer · Layered α -titanium phosphate · Ionic liquid

Introduction

Dye-sensitized solar cell (DSSC) has attracted considerable attention as a high-efficiency and low-cost alternative to conventional inorganic photovoltaic devices [1]. Generally, DSSC comprises a dye-sensitized nanocrystalline porous TiO₂ film immobilized on a transparent conducting oxide (TCO)-coated glass substrate, an electrolyte containing an I⁻/I₃⁻ redox couple, and a platinized TCO-coated glass substrate as the counter electrode. When the sensitizer dye absorbs solar energy, electrons are injected rapidly from the excited state of the dye into the conduction band of TiO₂. Injected electrons diffuse in TiO₂ and reach the outer circuit through the back contact. Oxidized dye molecules are reduced by I⁻ in the iodide-based liquid electrolyte via the reaction $3I^- \rightarrow I_3^- + 2e^-$, where I⁻ changes to I₃⁻ by losing two electrons. At the counter electrode, the reverse reaction takes place, where I₃⁻ is reduced to I⁻ by gaining two electrons from the counter electrode. In the iodide-based liquid electrolyte, I⁻ diffuses from the counter electrode to the dye, and I₃⁻ diffuses from the dye to the counter electrode. Among the above reactions, both the charge-transfer process at the Pt/electrolyte interface and the diffusion process of I₃⁻ in the electrolyte depend on the properties of the electrolyte. Therefore, the electrolyte plays an important role in the photovoltaic performance of DSSC by affecting the kinetics of electronic or ionic processes [2–4].

Although an impressive 11% light-to-electricity conversion efficiency has been obtained for photovoltaic devices with organic solvent-based electrolytes [5], these volatile organic solvents are of questionable durability due to their evaporation and leaking, especially for DSSC with a flexible matrix. Recently, room temperature ionic liquids have attracted growing attention due to their negligible

P. Cheng (✉) · R. Chen · J. Wang · J. Yu · T. Lan ·
W. Wang · H. Yang · H. Wu
National Key Laboratory of Nano/Micro Fabrication
Technology, Key Laboratory for Thin Film and Microfabrication
of the Ministry of Education, Research Institute of Micro/Nano
Science and Technology, Shanghai Jiao Tong University,
Shanghai 200240, People's Republic of China
e-mail: pcheng2008@sjtu.edu.cn

C. Deng
State Key Lab of New Ceramics and Fine Processing,
Institute of Nuclear & New Energy Technology,
Tsinghua University, Beijing 100084,
People's Republic of China

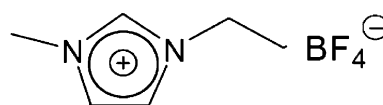
vapor pressure and high ionic conductivity [6–8]. They had the advantage of keeping their stability for a long time because ionic liquid electrolytes do not evaporate in normal temperature. However, the energy conversion efficiency could not reach that of DSSCs using volatile liquid electrolytes. This was mainly because that the viscosity of the ionic liquids was higher than that of volatile liquid solvents, which resulted in the low diffusion constant of I_3^- in the electrolyte and the large charge-transfer resistance at the counter electrode/electrolyte interface [9, 10].

Recently, many efforts have been made to improve the photovoltaic properties and the stability of DSSC filled with ionic liquid-based electrolyte by adding silica nanoparticles, carbon nanotubes, carbon nanoparticles and titanium dioxide nanoparticles into various ionic liquid electrolytes [11, 12]. Wang et al. reported that layered α -zirconium phosphate enhanced the exchange current density and the diffusion coefficient of triiodide in the electrolyte [13]. These striking and significant observations have triggered our interest to explore new layered materials to improve the electrochemical performances of the electrolyte and the photovoltaic characteristics of DSSCs. Crystalline α -titanium phosphate (α -TiP) has a two-dimensional layered structure similar to that of layered α -zirconium phosphate [14]. However, for layered α -TiP, P atoms in the lower sandwich lie along a perpendicular line drawn from the Ti atom of the upper sandwich. This arrangement renders it with larger inter-laminar cavities and a greater ion exchange capacity than α -zirconium phosphate [15]. The enlarged spacing would facilitate the diffusion of I_3^- in the ionic liquid electrolyte, thus enhancing the photovoltaic performance of DSSC. In addition, α -TiP has the common Ti ions with TiO_2 photoanode, which can avoid the possible effect of foreign zirconium ions on the photovoltaic characteristics of DSSC. Here, we firstly reported a composite electrolyte prepared by adding α -titanium phosphate (α -TiP) into 1-ethyl-3-methylimidazolium tetrafluoroborate (EmimBF₄) ionic liquid-based electrolyte showing a lower melting point and a higher conductivity [16]. The composite electrolyte exhibited very good electrochemical and photovoltaic properties.

Experimental

Sample Preparation

The synthesis of ionic liquid, 1-ethyl-3-methylimidazolium tetrafluoroborate (EmimBF₄) was carried out according to methods reported [17] with a molecular structure shown in Scheme 1. Crystalline layered α -TiP ($Ti(HPO_4)_2$) was prepared by the following processes. Under vigorous stirring



Scheme 1 Molecular structure of EmimBF₄ ionic liquid

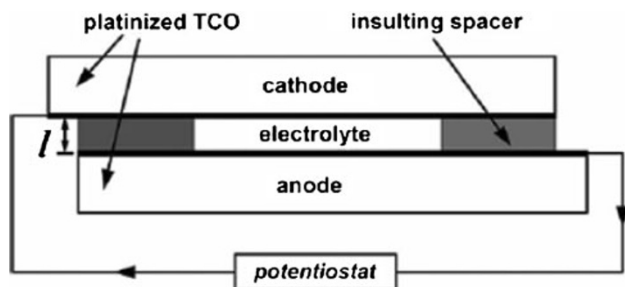
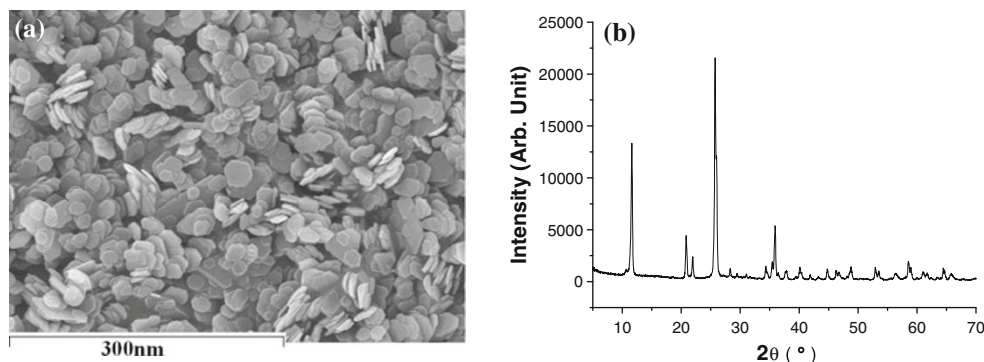
in the air, 8.5 g tetra-tert-butyl orthotitanate ($Ti(OC_4H_9)_4$, Beijing Chemical Reagent Co., Ltd) was slowly added to distilled water (50 ml). A white precipitate formed immediately upon addition of the tetra-tert-butyl orthotitanate. The precipitate was filtered and washed three times with distilled water. The filter cake was transferred to a Teflon™ titanium autoclave containing 9.8 g phosphoric acid solution (85 wt%) and 10 ml distilled water and then heated at 150°C for 16 h. The colloids were repeatedly washed with distilled water by centrifuging until the pH value of the solution was above 4. The final α -TiP powders was obtained after drying at 50°C for 24 h, with a yield of more than 90%. The morphology was shown in Fig. 1. The composite electrolytes were prepared by adding 0.5, 1 wt%, 1.5 and 2 wt% layered α -TiP powders relative to the electrolyte into the ionic liquid-based electrolyte (0.3 M LiI and 0.03 M I_2 in EmimBF₄ solvent) under ultrasonication for 2 h, respectively.

The setup used for electrochemical measurements was designed to be a symmetric thin-layer cell similar to the literature [4], as shown in Scheme 2. This electrochemical cell consisted of two identical platinized, TCO-coated glass substrates sealed with a Surlyn film (30 μ m thick, DuPont), which served as a spacer. The cell was filled with the composite electrolyte with various weight percentage of layered α -TiP. The TCO substrate used was F-doped SnO_2 (FTO) with a sheet resistance of 20 ohm/square. All measurements were carried out at room temperature. Dye-sensitized solar cell was composed of a dye-coated TiO_2 film (8 μ m thick) photoanode, platinized counter electrode, a surlyn spacer (30 μ m thick). The TiO_2 film was prepared according to the reported process [18]. And the composite electrolyte with various contents of α -TiP was introduced into the space of inter-electrodes through the two holes predrilled on the back of the counter electrode. The TiO_2 electrode was dipped into a dry ethanol containing 2.5×10^{-4} M N3 dye at room temperature for 20 h to realize sensitization. The active area of DSSC was 0.194 cm².

Characterization

Electrochemical impedance spectra (EIS) were measured using an IM6/IM6e (Zahner, Germany) electrochemical analyzer in a two-electrode configuration. A 10 mV AC perturbation was applied and the frequency range was 0.01 Hz–100 kHz. The limiting current density was determined by steady-state current–voltage curve of the Pt

Fig. 1 **a** SEM morphology and **b** XRD pattern of layered α -TiP nanoparticles



Scheme 2 The electrochemical cell used for the electrochemical measurements

thin-layer cell. The scan rate was 10 mV/s. Morphology of α -TiP powders was determined by field emission scanning electron microscope (FESEM, JEOL JSM-6301F). X-ray diffraction (XRD, RIGAKU D/MAX-2400) was used to characterize the crystal structure and interlayer distance of α -TiP crystalline. Photocurrent-voltage curves were recorded using a source meter (Keithley-2400, Keithley Co. Ltd., USA) under an illumination of 100mW/cm² (globe AM1.5, 1sun) from a Xenon lamp (Oriel) at room temperature.

Results and Discussion

Figure 1a showed the FESEM images of layered α -TiP nanoparticles. It can be seen that the particles were predominantly hexagonal platelet shaped with an average diameter of about 20 nm and an average thickness of about 3 nm. Figure 1b showed wide-angle XRD pattern of layered α -TiP nanoparticles. From the corresponding characteristic 2θ values of the diffraction peaks in Fig. 1b, it was confirmed that the as-prepared sample was identified as α -TiP phase (JCPDS 80-1067).

The Influence of α -TiP on the Charge-Transfer Resistance of R_{ct}

Figure 2 showed the electrochemical impedance spectra of the EmimBF₄-based composite electrolytes with various

contents of layered α -TiP, measured with the device in Scheme 2 at room temperature. All of the impedance spectra consisted of a semicircle at the high frequency region of the spectra and an inclining line after the arc, which were related to the reaction at Pt/electrolyte interface and the diffusion process of species in the electrolytes, respectively. The equivalent circuit given in Fig. 3 was used for the curve fitting of the impedance spectra. R_s is the ohmic serial resistance that includes both the sheet resistance of the FTO glass and the resistance of electrolyte, R_{ct} and C_{dl} are the charge-transfer resistance and double-layer capacitance at the Pt/electrolyte interface, respectively, and Z_w is the Warburg diffusion impedance. The curve fitting was carried out with Z-view software (Scribner Associate, Inc.). To compensate for the roughness of the electrode surface, constant phase elements (CPE) were used in the model in place of a capacitor keeping the exponent CPE-P quite close to the perfect capacitor value, CPE-P \approx 1. The fitted results were listed in Table 1. As shown in Table 1, the value of R_s for all the electrolytes were almost the same indicating the addition of layered α -TiP had little effect on the ionic conductivity of EmimBF₄-based electrolyte. The

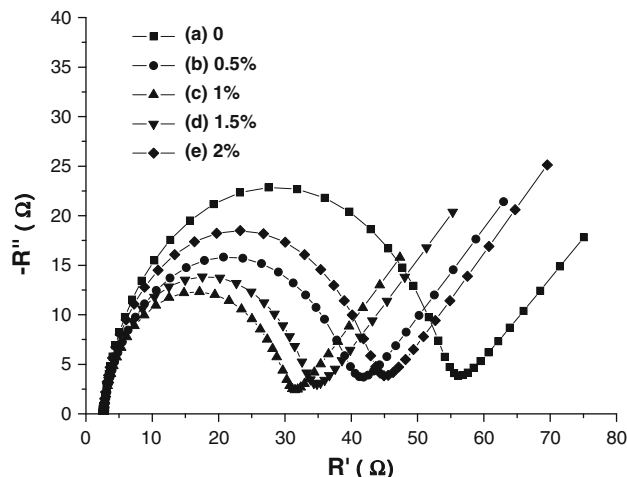


Fig. 2 Nyquist plots of electrochemical cell with various contents of α -TiP: **a** blank; **b** 0.5 wt%; **c** 1 wt%; **d** 1.5 wt%, and **e** 2 wt%

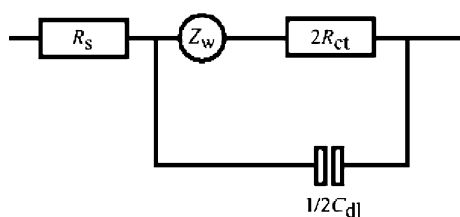


Fig. 3 Equivalent circuit for the electrochemical cells. R_s : ohmic serial resistance; R_{ct} : charge-transfer resistance; C_{dl} : capacitance of electrical double layer; Z_w : Warburg impedance

Table 1 Fitted parameters of the EmimBF₄-based electrolytes with various contents of layered α -TiP

Content of α -TiP (wt%)	R_s (Ω)	R_{ct} (Ω)	$Z_w(R)$ (Ω)
0	2.63	25.25	1.35
0.5	2.62	18.75	1.1
1	2.65	13.60	0.65
1.5	2.64	15.00	0.95
2	2.67	19.90	1.25

R_{ct} value decreased markedly with the increase in α -TiP content and a minimum of 13.60 Ω was achieved when the α -TiP content was 1wt%. The decrease of R_{ct} value revealed the enhanced electron-transfer reaction in the electrolyte, resulting from less energy loss at the Pt/electrolyte interface for the reduction of I_3^- to I^- , which would lead to an improved photovoltaic performance of DSSC. However, further increase in α -TiP content (>1wt%) led to an increase in R_{ct} . Although the value of Z_w was correlated to the diffusion coefficients of ions, it could only be used for qualitative analysis due to its small effect on the impedance spectra for the electrolytes with a high viscosity. So the exact diffusion coefficients should be determined from diffusion-limited currents, which were given in the following section.

The Influence of Layered α -TiP on the Diffusion Coefficient of I_3^-

Diffusion-limited currents of the thin-layer cells (Scheme 2) filled with the composite electrolytes containing various contents of layered α -TiP were determined by measurements of cyclic voltammograms. Steady-state current could be achieved for all the thin-layer cells. Figure 4 showed a typical steady-state I - V curves for the electrolyte without α -TiP. Due to the large excess of I^- relative to I_3^- , only the diffusion of I_3^- limited the current [3]. Therefore, diffusion coefficients of I_3^- ions (DI_3^-) in the electrolytes could be determined from the limiting current density (j_{lim}) by the following equation [19]:

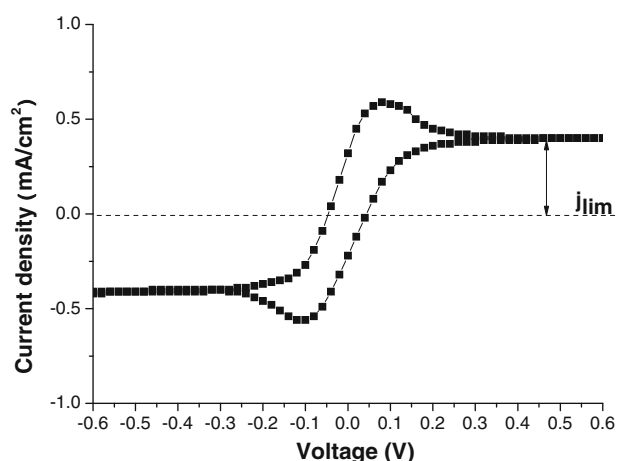


Fig. 4 Steady-state I - V curves of the electrochemical cell shown in Scheme 2. The electrolyte consisted of 0.3 M LiI, 0.03 M I_2 in EmimBF₄ solvent without α -TiP

$$DI_3^- = j_{lim}L/2nFC_{I_3^-}$$

where n is the number of electrons transferred in each reaction (here $n = 2$), L is the distance between the two electrodes (here $L = 30 \mu\text{m}$) and $C_{I_3^-}$ is the concentration of I_3^- (here $C_{I_3^-} = 0.03 \text{ M}$). The j_{lim} values and the corresponding DI_3^- values for the iodide-based composite electrolytes with various contents of α -TiP were summarized in Table 2. It could be observed that the diffusion coefficient of I_3^- was improved by the addition of α -TiP and a maximum of 1.515 mA/cm² was achieved when the content of α -TiP was 1wt%. Correspondingly, the maximum DI_3^- of the composite electrolyte was $3.93 \times 10^{-7} \text{ cm}^2/\text{s}$, which was twice more than the electrolyte without α -TiP. It was interesting that the variational tendency of DI_3^- with the α -TiP content was very consistent with that of charge-transfer reaction, which indicated that the optimal content of layered α -TiP was 1wt% in this study.

The Mechanism for the Improved Electrochemical Properties

α -TiP crystalline has a two-dimensional layered structure, as shown in Fig. 5a. The layered structure of α -TiP is built

Table 2 Limiting current density (j_{lim}) and diffusion coefficient (DI_3^-) for EmimBF₄-based electrolyte with various contents of layered α -TiP

Content of α -TiP (wt%)	j_{lim} (mA/cm ²)	DI_3^- ($10^{-7} \text{ cm}^2/\text{s}$)
0	0.401	1.04
0.5	0.805	2.08
1	1.515	3.93
1.5	1.123	2.91
2	0.575	1.49

up by bonding together the sandwiches through van der Waals forces. In this arrangement, each P atom in the lower sandwich lies along a perpendicular line drawn from the Ti atom of the upper sandwich. This arrangement makes it have larger interlamellar cavities and greater ion exchange capacities than other layered materials, such as α -zirconium phosphate, α -stannum phosphate and clay minerals [13, 15, 20, 21]. Hydrogen ions between the sandwiches could be exchanged by other cations, which would result in the pillared layered structure [22, 23].

In order to explore the mechanism for the improved electrochemical properties upon the addition of layered α -TiP, XRD experiments were carried out to characterize the interlayer distances of pristine and Emim⁺ pillared layered α -TiP. Excess EmimBF₄ ionic liquid was mixed with α -TiP powders under ultrasonication. The obtained suspension was centrifuged to form precipitate, and the filter cake was repeatedly washed with distilled water. After drying at 80°C for 24 h under vacuum, the white powder of pillared α -TiP was obtained. Figure 6 illustrated the low-angle XRD patterns of pristine and pillared layered α -TiP. For pristine α -TiP crystalline (Fig. 6a), the interlayer distance was indicated by the diffraction peak at $2\theta = 11.62^\circ$, corresponding to (002) plane. For pillared α -TiP, the peak of (002) plane was shifted from 11.62° to 8.38° , corresponding to the change of the interlayer distance from 7.6\AA to 10.5\AA , which indicated successful pillaring of α -TiP. The increased interlayer distance of 2.9\AA was almost equivalent to the size of Emim⁺ cation, which indicated that Emim⁺ cations exchanged with H⁺ ions between the sandwiches of α -TiP crystalline and were intercalated into the interspace of α -TiP to form Emim⁺ pillared layered α -TiP since Emim⁺ cation had the larger size than H⁺ ion, as illustrated in Fig. 6b. Similar result was reported for layered montmorillonite, which was intercalated by Emim⁺ cations through the ion exchange reaction [24]. It was reported that I₃⁻ ions in the solution take symmetrical linear form, with a diameter of about 2.9

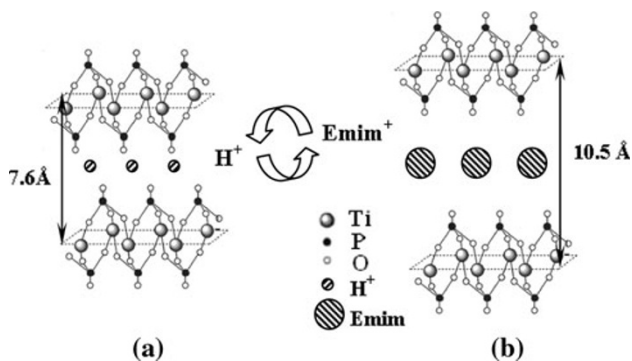


Fig. 5 Molecular structure of pristine (a) and pillared (b) layered α -TiP crystalline

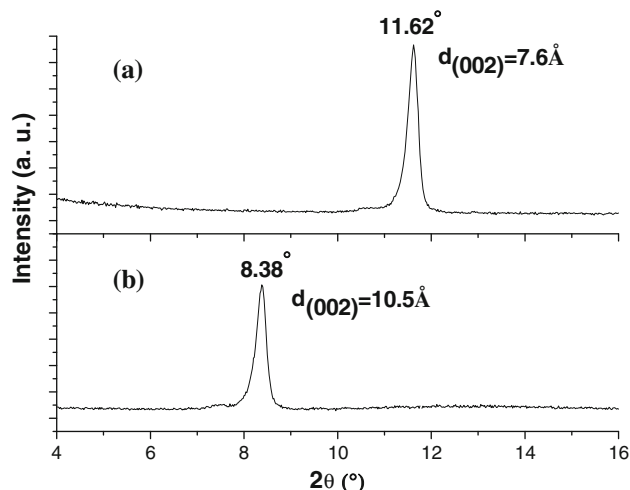


Fig. 6 XRD patterns of pristine (a) and Emim⁺ pillared (b) layered α -TiP

\AA and a length of about 5.8\AA , respectively [25]. For pristine α -TiP, the diameter of zeolite type cavities between the sandwiches is around 2.6\AA [15], which is small for I₃⁻ to transport through the interspace between the sandwiches of α -TiP. However, for the Emim⁺-pillared α -TiP, the interlayer distance is up to 10.5\AA , corresponding to the diameter of cavities up to 5.5\AA , which indicates that I₃⁻ ions can transport freely in a straight line through the interspace between the sandwiches of α -TiP. The nanochannels between the sandwiches of α -TiP would not only provide a fast diffusion path but also confine the transport direction of I₃⁻ ions, both of which could increase the steady-state current, thus the diffusion coefficient. Therefore, the confinement effect [26] by the nanochannels between the sandwiches of layered α -TiP was proposed to be responsible for the enhanced diffusion coefficient of I₃⁻ in the electrolyte. At the same time, α -TiP platelets would pile up to form the bridges between the two Pt electrodes. Then, charge transfer could also be partly carried out at the α -TiP/electrolyte interface beside at the Pt electrode/electrolyte interface. The active area of α -TiP/electrolyte interlamellar interface for charge-transfer reaction increased with the increase in α -TiP content due to the formation of more Emim⁺-pillared layered α -TiP, which resulted in the improved charge-transfer reaction, thus the decreased charge-transfer resistance R_{ct} . In addition, it was reported that the charge-transfer resistance at the Pt electrode/electrolyte interface was inversely proportional to the square root of the I₃⁻ concentration around the Pt/electrolyte interface [3]. In this study, the enhanced diffusion of I₃⁻ would lead to the higher local I₃⁻ concentration around the Pt/electrolyte interface, which also resulted in the decrease of R_{ct} . Therefore, both the increased active area of α -TiP/electrolyte interface and the higher local

concentration of I_3^- around the Pt/electrolyte interface contributed to the enhanced charge-transfer reaction as a function of α -TiP content.

However, when the α -TiP content was above 1wt%, both the diffusion of I_3^- and charge-transfer reaction were suppressed with the increase in the α -TiP content, which might be explained by the following two aspects. On one hand, excess α -TiP probably exhausted all the $Emim^+$ ions in the electrolyte and no more $Emim^+$ -pillared α -TiP could be formed. On the other hand, excess α -TiP powders would increase the viscosity of the electrolyte to some extent. Both the aspects described previously are harmful and would counteract the diffusion of I_3^- and the charge transfer. Therefore, the optimal content of α -TiP was 1wt% in this study, where the diffusion of I_3^- and the charge transfer were the most efficient.

The Influence of Layered α -TiP on the Photovoltaic Performance of DSSC

Figure 7 showed the photocurrent-voltage characteristic curves of DSSCs based on the electrolytes with various contents of α -TiP. The corresponding photovoltaic characteristic parameters of DSSCs were summarized in Table 3. The conversion efficiency η was markedly enhanced by the addition of layered α -TiP and the maximum was achieved when the content of α -TiP was 1wt%, where both J_{sc} and V_{oc} reached their maximum. The improved photocurrent J_{sc} with increasing α -TiP content was attributed to the improved diffusion coefficient of I_3^- and the reduced charge-transfer resistance, as described in the previous sections. It has been reported that the relation

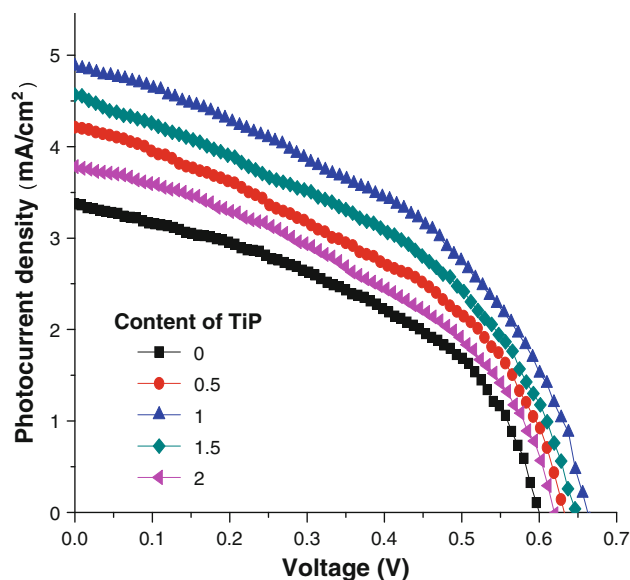


Fig. 7 Photocurrent-voltage characteristic curves of DSSCs with various contents of layered α -TiP

Table 3 Photovoltaic parameters of DSSCs based on the composite electrolytes with various contents of layered α -TiP

Content of TiP (wt%)	J_{sc} (mA/cm ²)	V_{oc} (V)	FF	η (%)
0	3.372	0.599	0.44	0.90
0.5	4.211	0.632	0.43	1.13
1	4.880	0.662	0.44	1.43
1.5	4.565	0.646	0.43	1.26
2	3.78	0.619	0.42	0.99

between open circuit (V_{oc}) of DSSC and concentrations of I_3^- and oxidized dyes (D^+) was expressed as follows [27, 28]:

$$V_{oc} = \frac{RT}{nF} \ln \left(\frac{AI}{n_0 k_1 C I_3^- + n_0 k_2 C D^+} \right)$$

where k_1 , k_2 , and I are kinetic constants of recombination of the injected electrons with I_3^- , with oxidized dyes (D^+), and incident photon flux, respectively. And n_0 is the concentration of accessible electronic states in the conduction band. It was apparent that the open circuit voltage V_{oc} was inversely proportional to k_1 , k_2 , $C_{I_3^-}$ and C_{D^+} . Under illumination, I_3^- ions produced in situ by dye regeneration diffused to the counter electrode. The improved diffusion coefficient of I_3^- resulted in the decreased local I_3^- concentration around TiO_2 nanoparticles and would slow down the possible charge recombination between the injected electrons and I_3^- at TiO_2 /electrolyte interface. According to the equation, the V_{oc} value increased when the recombination kinetic constant of k_1 decreased. Therefore, when the content of α -TiP was below 1wt%, the photocurrent J_{sc} , the open circuit voltage V_{oc} and hence the conversion efficiency η of DSSC increased with increasing α -TiP content. However, when the content of α -TiP was above 1 wt%, J_{sc} , V_{oc} and hence η decreased with increasing α -TiP content, which probably resulted from the decreased diffusion coefficient of I_3^- and the increased charge-transfer resistance.

Conclusions

In summary, we reported a composite electrolyte prepared by incorporating layered α -titanium phosphate into $EmimBF_4$ -based electrolyte, which exhibited excellent electrochemical and photovoltaic properties. The charge-transfer reaction at the Pt/electrolyte interface and the diffusion coefficient of I_3^- in the electrolyte were both enhanced markedly, both of which was ascribed to the intercalation behavior of $Emim^+$ cations into layered α -TiP. The confinement effect by the nanochannels between the sandwiches of layered α -TiP was proposed to be responsible for the enhanced diffusion

coefficient of I_3^- in the electrolyte. The increased active area of α -TiP/electrolyte interface and the higher local concentration of I_3^- around the Pt/electrolyte interface might contribute to the improved charge-transfer reaction. The optimum of 1 wt% α -TiP was obtained for the EmimBF₄-based electrolyte, where both the diffusion of I_3^- , the charge-transfer reaction and photoelectric conversion efficiency were the most efficient. These quasi-solid-state electrolytes offer a broad prospect for the application of ionic liquids in DSSC. They will enable the fabrication of flexible, compact, laminated solid-state devices free of leakage and available in various geometries.

Acknowledgments The authors acknowledge financial support from National Nature Science Foundation of China (50802051), National High Technology Research and Development Program of China (863 Program, 2006AA03Z218) and China Postdoctoral Science Foundation (20060400055).

Open Access This article is distributed under the terms of the Creative Commons Attribution Noncommercial License which permits any noncommercial use, distribution, and reproduction in any medium, provided the original author(s) and source are credited.

References

1. M. Grätzel, *Nature* **414**, 338 (2001)
2. J. Ferber, R. Stangl, J. Luther, *Sol. Energy Mater. Sol. Cells* **53**, 29 (1998)
3. A. Hauch, A. Georg, *Electrochim. Acta* **46**, 3457 (2001)
4. N. Papageorgiou, W.F. Maier, M. Grätzel, *J. Electrochem. Soc.* **144**, 876 (1997)
5. M.K. Nazeeruddin, P. Pechy, T. Renouard, S.M. Zakeeruddin, R. Humphry-Baker, P. Comte, P. Liska, L. Cevey, E. Costa, V. Shklover, L. Spiccia, G.B. Deacon, C.A. Bignozzi, M. Grätzel, *J. Am. Chem. Soc.* **123**, 1613 (2001)
6. R.D. Rogers, K.R. Seddon, *Science* **302**, 792 (2003)
7. J. Dupont, R.F. de Souza, P.A.Z. Suarez, *Chem. Rev.* **102**, 3667 (2002)
8. W. Kubo, T. Kitamura, K. Hanabusa, Y. Wada, S. Yanagida, *Chem. Commun.* **374**, 56 (2002)
9. P. Wang, B. Wenger, R. Humphry-Baker, J.E. Moser, J. Teuscher, W. Kantlehner, J. Mezger, E.V. Stoyanov, S.M. Zakeeruddin, M. Grätzel, *J. Am. Chem. Soc.* **127**, 6850 (2005)
10. D.B. Kuang, P. Wang, S. Ito, S.M. Zakeeruddin, M. Grätzel, *J. Am. Chem. Soc.* **128**, 7732 (2006)
11. P. Wang, S.M. Zakeeruddin, P. Comte, I. Exnar, M. Grätzel, *J. Am. Chem. Soc.* **125**, 1166 (2003)
12. H. Usui, H. Matsui, N. Tanabe, S. Yanagida, *J. Photochem Photobiol. A. Chem.* **164**, 97 (2004)
13. N. Wang, H. Lin, X. Li, C.F. Lin, L.Z. Zhang, J. Wu, Y. Dou, J.B. Li, *Electrochem. Commun.* **8**, 946 (2006)
14. A. Clearfield, U. Costantino, in *Comprehensive supramolecular chemistry*, ed. by G. Alberti, T. Bein (Pergamon Press, New York, 1996)
15. K.M. Parida, B.B. Sahu, D.P. Das, *J. Colloid Interface Sci.* **270**, 436 (2004)
16. R. Kawano, H. Matsui, C. Matsuyama, A. Sato, M. Susan, N. Tanabe, M. Watanabe, *J. Photochem. Photobiol. A* **164**, 87 (2004)
17. K. Matsumoto, R. Hagiwara, R. Yoshida, Y. Ito, Z. Mazej, P. Benkic, B. Zemva, O. Tamada, H. Yoshino, S. Matsubara, *Dalton Trans.* **144**, 96 (2004)
18. P. Cheng, C.S. Deng, X.M. Dai, B. Li, D.N. Liu, J.M. Xu, *J. Photochem. Photobiol. A-Chem.* **195**, 144 (2008)
19. N. Papageorgiou, Y. Athanossos, M. Armand, P. Bonhote, H. Pettersson, A. Azam, M. Grätzel, *J. Electrochem. Soc.* **143**, 3099 (1996)
20. C.B. Amphlett, *Inorganic ion exchangers* (Elsevier, Amsterdam, 1964)
21. A. Clearfield, G.D. Smith, *J. Inorg. Chem.* **8**, 431 (1969)
22. D.P. Das, K.M. Parida, *Appl. Catal. A-Gen.* **324**, 1 (2007)
23. L. Szirtes, L. Riess, J. Megyeri, E. Kuzmann, *Cent. Eur. J. Chem.* **5**, 516 (2007)
24. N.H. Kim, S.V. Malhotra, M. Xanthos, *Microporous Mesoporous Mat.* **96**, 29 (2006)
25. H. Sakane, T. Mitsui, H. Tanida, I. Watanabe, *J. Synchrotron Radiat.* **8**, 674 (2001)
26. S.H. Anastasiadis, K. Karatasos, G. Vlachos, E. Manias, E.P. Giannelis, *Phys. Rev. Lett.* **84**, 915 (2000)
27. Q. Wang, J.E. Moser, M. Grätzel, *J. Phys. Chem. B* **109**, 14945 (2005)
28. M. Koelsch, S. Cassignon, C.T.T. Minh, J.F. Guillemoles, J.P. Jolivet, *Thin Solid Films* **451–452**, 86 (2004)